Characteristics of Microencapsulated PCM Slurry as a Heat-Transfer Fluid

Yasushi Yamagishi
Daido Hoxan Inc., Osaka 592, Japan

Hiromi Takeuchi and Alexander T. Pyatenko
Hokkaido National Industrial Research Institute, Sapporo 062, Japan

Naoyuki Kayukawa
Center for Advanced Research of Energy Technology, Hokkaido University, Sapporo 060, Japan

The hydrodynamic and heat-transfer characteristics of slurry containing microencapsulated phase-change materials (MCPCMs) were investigated experimentally for use as a heat-transfer fluid. Pressure drop and local convective heat-transfer coefficients of the slurry flows in a circular tube with uniform heat flux were measured. Slurries consisting of octadecane ($C_{18}H_{38}$) contained in 2−10-μm-dia. microcapsules and pure water were used. The particle volume fractions in the slurry were varied up to 0.3. Results showed that increases in particle volume fractions caused the slurry flow structure to change from turbulent to laminar, and the pressure-drop reduction of the slurry flow relative to a single-phase water flow was under the same flow-rate conditions. The heat-transfer performance of the slurry also depended on the change in flow structure. When the MCPCMs melted, the local heat-transfer coefficients for turbulent slurry flows increased relative to those for nonmelting slurry. This phenomenon was influenced by the MCPCM fraction, the degree of turbulence, and the heating rate at the tube wall. The experimental data will be useful in the design of thermal-energy transportation systems using MCPCM slurry.

Introduction

Many thermal-energy systems have long sections of piping to convey heat-transfer fluids between the heat exchangers for source and sink. In such conventional systems, thermal energy is transferred by the sensible heat of a single-phase working fluid, being proportional to the source−sink temperature difference. Because the systems are often operated with small temperature differences, the single-phase fluid must be pumped at a high-volume flow rate. As a result, the system consumes a large amount of pumping power. The increase in the thermal capacity of heat-transfer fluid is an important problem and is of growing concern to engineers.

The use of phase-change material (PCM) particles suspended in a single-phase working fluid would provide additional thermal capacity from the latent heat associated with the solid−liquid phase change. Several methods for generating PCM particles have been investigated for various thermal-energy applications. For district cooling systems, an ice-water slurry has been developed and is implemented in practice. Cleary et al. (1990) found that ice slurry of 25% in particle volume concentration had a thermal capacity that was 2 to 4 times higher than that of chilled water. Choi et al. (1994) developed a system that generated solid hexadecane ($C_{16}H_{34}$) particles of 0.1 mm in size, using an emulsifier, and they studied the heat-transfer characteristics of the hexadecane−water slurry. However, because such particles of nonencapsulated PCMs are slightly sticky and can stick together to form large lumps, clogging often occurs in a piping system, resulting in failure to circulate the slurry through the system (Winters, 1991). In addition, such systems require rel-

Correspondence concerning this article should be addressed to Y. Yamagishi.

atively large equipment for generating the particles, which results in an associated large capital investment for the system. The purpose of the present study was to investigate the feasibility of using a slurry of microencapsulated phase-change material (MCPCM) as a heat-transfer fluid. Besides the benefit of the additional thermal capacity, no special equipment for generating PCM particles is needed because the PCM is always separated from the suspending fluid. Therefore, this type of slurry can be treated as a conventional single-phase working fluid.

In previous works, efforts have been made to manufacture MCPCMs with sufficient strength (Hart and Thornton, 1982; Roy and Sengupta, 1991). Several promising applications using MCPCM slurries as a heat-transfer and storage medium have been proposed (Mehalick and Tweedie, 1975; Baharami, 1982; McMahon et al., 1982; Colvin and Mulligan, 1986). Kasza and Chen (1985) presented the results of an analytical study on solar-energy or waste-heat utilization systems using MCPCM slurry and outlined the potential benefits of slurry as a heat-transfer fluid. They claimed that the convective heat-transfer coefficient for laminar and turbulent slurry flows would increase because of the increase in the effective specific heat, Cp_{eff}, and the effective thermal conductivity, k_{eff}.

One of the heat-transfer correlations for a fully developed turbulent flow of a single-phase fluid shows that the relationship between the Nusselt number, Nu, and the Prandtl number, Pr, is $Nu \sim Pr^{0.4}$ (Holman, 1981). Therefore, the convective heat-transfer coefficient, h, for a single-phase fluid can be described in terms of thermal conductivity, k, and specific heat, Cp, as

$$h \sim k^{0.6} Cp^{0.4}. \tag{1}$$

If the latent heat is viewed as a form of specific heat, the increase in effective specific heat Cp_{eff}, which includes the effect of latent heat, can lead to an increase in the heat-transfer coefficient, since Cp in Eq. 1 is replaced by Cp_{eff} (Kasza and Chen, 1985). Several experimental studies on laminar flows of MCPCM slurries were conducted to evaluate the effect of latent heat on heat-transfer coefficients (Chen and Chen, 1987; Colvin et al., 1992; Mulligan et al., 1994; Goel et al., 1994). Colvin et al. (1992) manufactured MCPCMs whose particle diameters ranged from one to several-hundred microns and measured the effective specific heat during phase change, which was defined as

$$Cp_{\text{eff}} = Cp + \epsilon c_{\text{pcm}} \lambda / \Delta T, \tag{2}$$

where c_{pcm} is the weight fraction of the PCM in the slurry; λ is the latent heat of PCM; ΔT is the difference between the slurry temperatures at the inlet and the outlet of a heat exchanger; and ϵ is the fraction of MCPCM particles that undergo phase change within the heat exchanger. They claimed that the average heat-transfer coefficients in the overall heat exchanger, which were calculated from the measured effective specific heat, was 50–100% higher than those for slurry with no phase change. Charunyakorn et al. (1990) developed a numerical simulation of the laminar slurry flow in a circular duct and predicted that the Nusselt number was 2 to 4 times higher than that of single-phase fluids. As for the effective thermal conductivity, k_{eff}, Sohn and Chen (1984) showed that the thermal conductivity of solid–liquid suspensions increased effectively in a laminar flow because of the effects of microconvection around solid particles and particle-to-particle interaction. The degree of the enhancement of thermal conductivity increases as particle diameter increases. For particle diameters smaller than 100 microns, however, this enhancement can be negligible. An associated heat-transfer enhancement is therefore believed to be marginal compared to those related to latent heat (Charunyakorn et al., 1990; Mulligan et al., 1994; Goel et al., 1994; Choi et al., 1994), although the effects on turbulent heat transfer have not yet been clarified. In addition, Choi et al. (1994) measured local pressure drops and local heat-transfer coefficients of turbulent slurry flow using the just-mentioned hexadecane– water slurry. They showed that both local pressure drop and local heat-transfer coefficient in a heated circular tube varied significantly along the flow direction when the solid hexadecane particles melted. They suggested that the effect of latent heat on the local heat-transfer coefficients may also depend upon the slurry flow structure. In the case of MCPCM slurry, on the other hand, there has been no experimental study on turbulent flow.

Experimental data on the thermodynamic and heat-transfer characteristics of either PCM or MCPCM slurry are still incomplete. In previous studies, the relationship between the hydrodynamics and the effect of latent heat on heat-transfer performance were not explored. The lack of a general and systematic study makes it difficult to interpret or evaluate many of the previous results. Consequently, the data necessary for engineering design of a thermal-energy system using MCPCM slurry are almost completely lacking. In this article, the results of pressure-drop measurement and local heat-transfer coefficients are presented for both turbulent and laminar slurry flows. First, the hydrodynamic characteristics, based on the pressure-drop data, are discussed. Then, the heat-transfer performance related to the hydrodynamic structures are presented. Finally, the desirable operating conditions of the system using MCPCM slurry are discussed.

Experimental

Microcapsules and slurry

Figure 1 is a photomicrograph of the MCPCM particles used in the present study. The particles consist of laboratory-grade octadecane ($C_{18}H_{38}$), with a melting temperature of 301 K and latent heat of 223 kJ/kg, and a melamine–formaldehyde resinous wall. The particle diameters were measured by using a laser light-scattering instrument (Leeds & Northrup Inc., Microtrac X-100) and were found to be in the range of 2–10 μm with a mean diameter 6.3 μm. The thickness of the coating wall was approximately 0.1 micron. Pure water was chosen as the suspending fluid for the MCPCM particles because it is easy to handle and does not react chemically with either octadecane or the coating material on the wall.

The structural stability of microcapsules during pumping was evaluated using capsules of various sizes in our preliminary study (Yamagishi et al., 1996). After repeated circula-

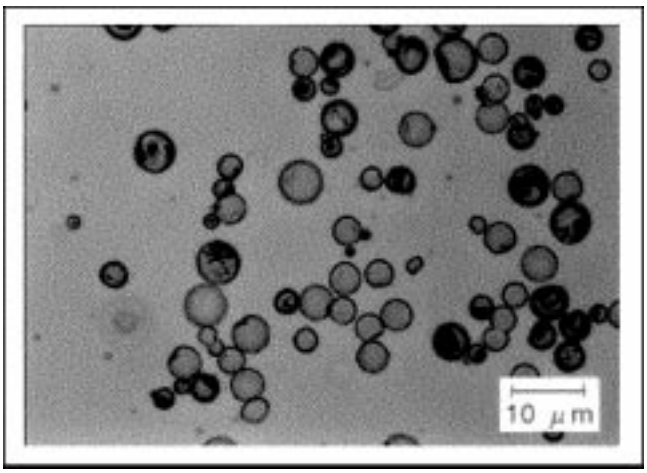

Figure 1. Photomicrograph of MCPCM slurry at 305 K.

tions through a slurry flow circuit, the breakage fractions of capsules with a smaller size were found to be lower. Capsules of 2–10 μm in diameter were suitable for this study because these microcapsules could be pumped without significant damage. In addition, thermal cycling across the PCM melting temperature, which caused mechanical stress to the coated wall associated with the volume change of PCM, did not damage the wall even at above 5,000 cycles, where one cycle included both melting and solidification processes.

Physical properties

Microencapsulating octadecane had no effect on its melting temperature or latent heat. These thermal properties of MCPCMs were found to remain constant after repeated thermal cycles. As reported elsewhere, however, microencapsulated PCMs often exhibit a supercooling phenomenon, that is, the solidification temperature of the MCPCM is lower than its melting temperature (Yamane, 1992; Roy and Sengupta, 1991). We investigated the supercooling phenomenon of MCPCM, and we reduced the degree of supercooling, which is defined as a difference between the melting and solidification temperatures, from 13 K to 5 K at a cooling rate of 5 K/min by adding a nucleating agent inside the capsules (Yamagishi et al., 1998a). The effect of supercooling on the measurement of local heat-transfer coefficients must be taken into account and will be described in a later section.

The density, specific heat, thermal conductivity, and latent heat of MCPCM slurry and its components are given in Table 1. These bulk physical properties are calculated from the combination of pure water, coating-wall material, and octadecane using the equations given in Appendix A. The weight fractions of wall-coating material and octadecane in the slurry were determined from the feed weight used in the slurry manufacturing process. The particle volume fraction, ϕ, in the slurry and the physical properties were estimated from these weight fractions. The weight ratios between the coating material and octadecane were the same for all the slurry samples. When the particle volume fraction is 0.3, the volume fraction of the coating material in the slurry is approximately 0.07. The physical properties of a MCPCM particle were calculated under the assumption that all of the particles had the same diameter (that is, $d_p = 6.3$ μm) and the coated walls all had the same thickness (that is, 0.1 μm). The values of slurry viscosity given in Table 1 were based on the pressure-drop experimental data, as is described in a later section.

Experimental apparatus and method

The pressure drops and the local convective heat-transfer coefficients were measured for the fluid flows of pure water and MCPCM slurry in a circular tube with uniform heat flux. The experimental apparatus is shown in Figure 2, the major components of which were two slurry reservoirs, a slurry pump, hydrodynamic entry and heat-transfer test sections, a mixing chamber, and an ac power supply. The pump was a Moyno progressive cavity pump, which was also used in the

Table 1. Physical Properties of MCPCM Slurry and Its Components

	Density $kg \cdot m^{-3}$	Specific Heat $J \cdot kg^{-1} \cdot K^{-1}$	Thermal Conductivity $W \cdot m^{-1} \cdot K^{-1}$	Latent Heat $kJ \cdot kg^{-1}$	Viscosity† mPa·s at 298 K
Octadecane* (Solid)	850	1,800	0.340	223	—
(Liquid)	780	2,200	0.150		
Melamine–formaldehyde**	1,490	1,670	0.420	—	—
Water (at 298 K)***	997	4,180	0.610	—	0.87
MCPCM particle (Solid)	1,000	1,754	0.310	167	—
(Liquid)	936	2,014	0.144		
MCPCM Slurry‡ (particle volume fraction)					
$\phi = 0.07$	998	4,009	0.597	10.2	1.17
$\phi = 0.12$	998	3,887	0.571	17.4	1.19
$\phi = 0.15$	998	3,824	0.566	21.8	2.26
$\phi = 0.25$	999	3,572	0.531	36.3	6.26
$\phi = 0.30$	989	3,489	0.483	43.6	10.4

*The Society of Thermophysical Properties (1994).
**Roff et al. (1971).
***JSME (1986).
†Slurry viscosities were estimated from pressure-drop data.
‡Bulk physical properties of slurries shown here are calculated from those of solid MCPCM particles.

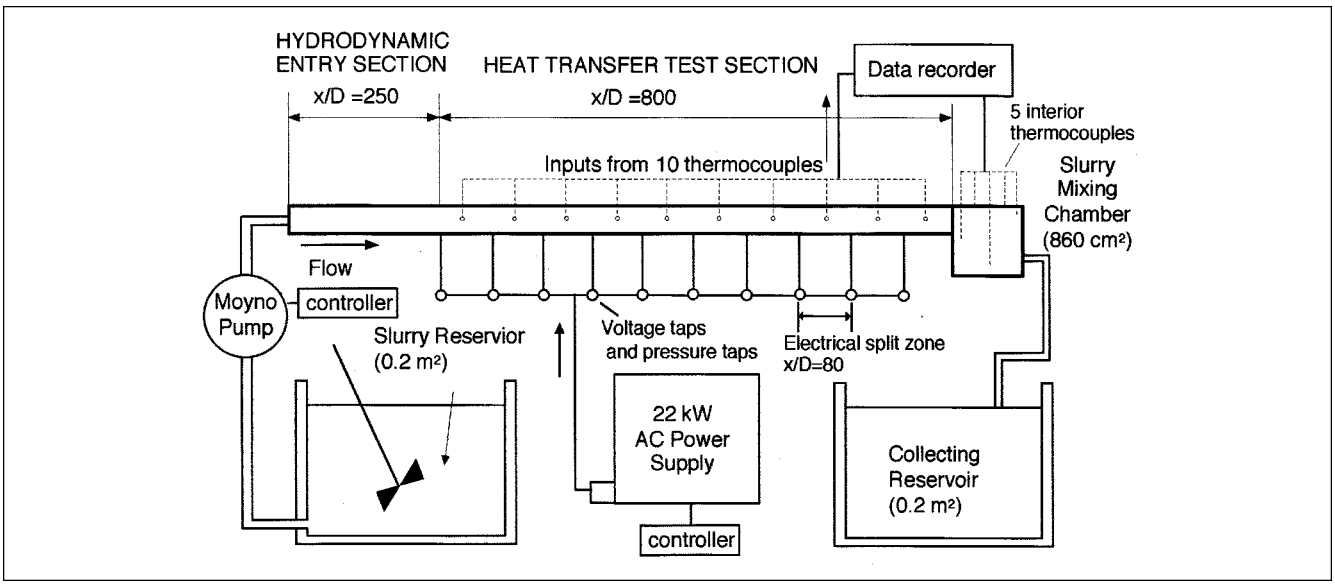

Figure 2. Experimental apparatus.

structural-stability test mentioned earlier. The hydrodynamic entry and heat-transfer test sections consisted of a single straight stainless-steel tube with an inner diameter, D, of 10.1 mm and wall thickness of 1.0 mm. The lengths of the hydrodynamics entry section and heat-transfer test sections were 2.5 and 8.0 m (250 and 800 times the diameter), respectively.

The local convective heat-transfer coefficient, h_x, between a fluid flow and the inner tube wall was defined as

$$h_x = \frac{q_{wx}}{T_{wx} + T_{bx}}, \tag{3}$$

where T_{bx} is the local bulk mean temperature, T_{wx} is the inner wall temperature, and q_{wx} is the local heat flux at the tube wall. In the case of pure water, the local bulk mean temperature can easily be estimated from a linear temperature rise along the test section under the condition of uniform heat flux. When no phase change is involved in the slurry, the temperature at any location in the test section can also be readily calculated. However, when a phase change occurs, the temperature rise across the melting temperature of octadecane is not linear because of latent heat.

To minimize uncertainty in the measurements of local bulk mean temperature, T_{bx}, during phase change, the test section was divided equally into ten segments (that is, 80 times the diameter of each). Each segment was wound with an insulated Nichrome-wire heater to apply a uniform heat flux to the tube wall. The diameter of the Nichrome wire was 0.58 mm. The electrical resistances of heaters were designed to be the same for all of the segments. Ten voltage taps were located at the end of each segment and were connected to the ac power supply in parallel. The mixing chamber was located just downstream of the test section to measure the temperature of effluent fluid from the test-section outlet. Five T-type thermocouples were immersed into this chamber. The test section and the mixing chamber were covered with glass-fiber wool to prevent heat loss. Each segment can be heated separately, and so the length of the heating part in the test section can be varied from the inlet to the outlet, with the remainder being thermally insulated. When a steady-state flow condition and a thermal equilibrium state of the experimental system were attained, the local bulk mean temperature at the end of variable-length heating part was calculated by the arithmetic mean of five temperature indications in the mixing chamber. The inner-wall temperature, T_{wx}, was estimated from the outer-wall temperature using a model for steady-state heat conduction (Holman, 1981). Ten T-type thermocouples were attached to the outer tube wall at the center position of each segment. The local bulk mean temperature at the center position was estimated by linear interpolation, including the temperatures at two adjacent ends of each segment.

The volume flow rates of the fluids, which were determined by measuring the volume of the effluent fluid, varied in the range of 4,000 to 7,500 cm^3/min. The mixing chamber had a capacity of 860 cm^3. Therefore, the residence time of the particles in the mixing chamber, which was defined as the ratio of the capacity of the chamber to the volume flow rate, was only on the order of 7−12 s. The system was judged to be in a thermal steady state when every five temperature indications in the chamber had settled to a desired slurry temperature within a fluctuation of ± 0.1 K for a period of at least 30 s. The maximum temperature difference among five thermocouples was less than 0.2 K in the thermal equilibrium state.

Ten pressure taps, as well as ten voltage taps, were located at the ends of the segments and connected to pressure transducers (Nagano Keiki Co., GC 62). All of fifteen thermocouples were calibrated by the ice point and steam point of pure water and the melting point of octadecane. Temperature and pressure data were acquired through a high-resolution data-acquisition system (Chino Co., LE 1000) and processed by a personal computer (NEC PC).

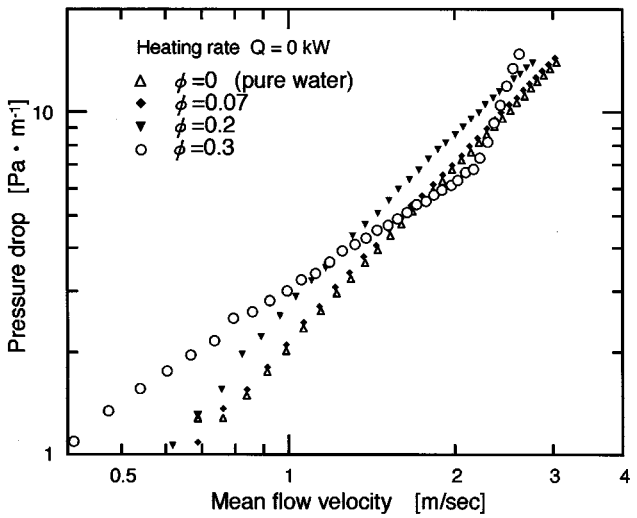

Figure 3. Pressure drop vs. mean flow velocity for pure water and MCPCM slurries at 298 K.

Results and discussion

Pressure drop measurement

Figure 3 shows the pressure drop per unit length for pure water and MCPCM slurries of several particle volume fractions, ϕ. These values were calculated from the pressure drops, $\Delta P > 0$, which were measured with a spacing, Δx, of 80 diameters from the test-section inlet when the heat flux was not applied. The fractions, ϕ, were varied up to 0.3. The temperatures of the fluids in the test section were below the melting temperature of octadecane ($T_b = 298$ K). As is shown in the figure, the pressure drops increase with the mean flow velocity, $\bar{u}$, which was calculated from the volume flow rate. When data at the same mean flow velocity are compared between pure water and slurries of $\phi = 0.07$ and 0.2, the pressure drops increase with the particle fractions. This can be attributed to the increased slurry viscosity according to the increasing particle fraction.

Figure 4 shows the relationship between friction factors, f, and Reynolds numbers, Re_b, for pure water and slurries of

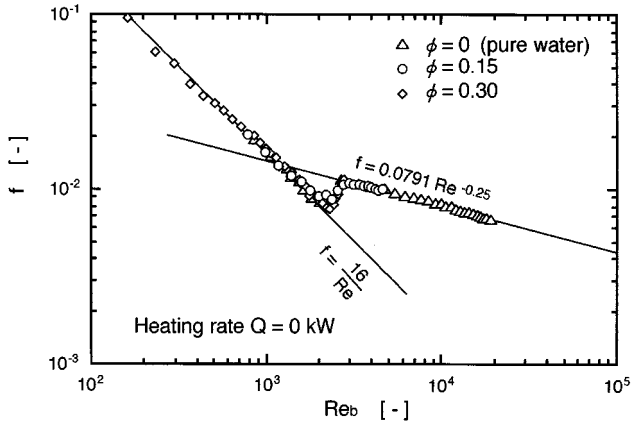

Figure 4. Friction factor vs. Reynolds number for pure water and MCPCM slurries at 298 K.

$\phi = 0.15$ and 0.3. The friction factor was defined as

$$f = (D\Delta P/\Delta x)/(2\rho_b \bar{u}^2). \quad (4)$$

In the case of pure water, the friction factors in Reynolds numbers of greater than 3,000 were in good agreement with the predicted values using Blasius equation. The average deviation of the experimental data from the predicted values was $+3.6\%$. The volume flow rates were checked repeatedly to confirm the existence of a steady-state flow condition, and the maximum deviation from the mean value was $\pm 5.0\%$. The transition from a laminar to turbulent flow occurred in the Reynolds number range of 2,000 to 3,000, which is in good agreement with the values cited elsewhere (that is, $Re_b \sim 2300$). In the case of MCPCM slurries, if there is no flocculation of particles and if the particles are completely dispersed in the slurry (that is, a homogeneous slurry), the slurry of such fine particles can be treated as a Newtonian homogeneous fluid, that is, the pressure drops in a laminar flow regime can be calculated as a linear function of the slurry viscosity (Darby, 1986; Aude et al., 1983). Based on this fact, the friction factors and Reynolds numbers for the slurry flows were calculated under the assumption that the slurries were Newtonian homogeneous fluids, where the Reynolds number for the slurry was defined using the slurry viscosity, η_b, as $Re_b = \rho_b \bar{u} D/\eta_b$. The slurry viscosities were estimated parametrically to fit the friction factors for the slurry flow to those for the Newtonian fluid with the same viscosity. The estimated viscosities are given in Table 1. As is shown in Figure 4, the friction factors in $Re_b < 2{,}000$ for all the slurries are fitted in those for Newtonian fluids, which were predicted on the basis of Hagen-Poiseuille theory (Schlichting, 1960). In the range of $Re_b > 3{,}000$, the friction factors of the slurry of $\phi = 0.15$ are approximately equal to those for pure water. Also, in the case of a slurry of $\phi = 0.3$, the friction factors increase in the range of $Re_b = 2{,}000-3{,}000$, which can be attributed to the change in flow structure from laminar to turbulent.

The slurries of very fine particles often exhibit non-Newtonian rheological behavior because of the flocculation of the particles. Eveson (1957) however, reported that the flocculation of the particles of 2−13 microns in size was impeded by a suitable dispersing agent. In the present study, an anionic surfactant of less than 1 wt. % was added to the slurries. According to our earlier study on MCPCM slurry rheology using the Couette (concentric cylinder) viscometer (Yamagishi et al., 1996), this surfactant was found to improve the degree of particle dispersion, and the non-Newtonian rheological behavior was not detected for the slurries of up to $\phi = 0.3$. It seems reasonable to suppose that the effect of non-Newtonian rheology on the slurry pipe flows of $\phi = 0-0.3$ is not significant. If this effect should be significant, it is difficult to apply such a linear approximation to the relationship between friction factors and slurry viscosities because the velocity profiles for a laminar non-Newtonian flow are different from those for a Newtonian flow (Dodge and Metzner, 1959). For a turbulent slurry flow, on the other hand, Park et al. (1995) found that there were no significant differences in the velocity profile or the longitudinal turbulent intensity between a non-Newtonian slurry with 2-micron silica-gel parti-

cles and a single-phase Newtonian fluid, where the slurry flow was investigated using a laser Doppler anemometer.

In the previous studies of laminar MCPCM slurry flows (Charunyakorn et al., 1990; Mulligan et al., 1994; Goel et al., 1994), the assumption of a Newtonian homogeneous slurry was also made to characterize the flow behavior and the relationship between the viscosities of MCPCM slurry, and the particle volume fractions, ϕ, were commonly modeled using one of the correlations for a slurry, which was described by the following equation (Vand, 1945):

$$\eta_s/\eta_f = \left(1 - \phi - A\phi^2\right)^{-2.5}. \qquad (5)$$

where η_s and η_f were the viscosities of the slurry and the suspending fluid, respectively. The constant, A, which depends upon the shape and rigidity of the particles, can be determined experimentally. Mulligan et al. (1994) employed Eq. 5 for the slurry with the MCPCM particles of 10–30 μm in size and obtained the value $A = 3.4$. In the present study, the slurry viscosities for $\phi = 0.1$–0.2 were estimated to be approximately 1.5 to 3 times higher than the viscosity of pure water. For $\phi = 0.3$, the viscosity was estimated to be about 12 times higher. As a result, the value $A = 3.7$ was obtained from these viscosities, although the estimated viscosity would be an effective value that includes the effect of interaction between particles, the suspending fluid, and the tube wall. The estimated viscosities increased nonlinearly with particle volume fractions.

Figure 5 shows the relationship between temperature and apparent viscosity for the MCPCM slurry of $\phi = 0.15$, measured using a Couette viscometer (Toki Sangyo Co., RB 100). In this measurement, the gap size between the inner and outer cylinders was 1.27 mm, and the shear rate was 100 s^{-1}. The apparent viscosity of the slurry approximately coincides with the viscosity given in Table 1. The relative viscosity, which is defined as the ratio of the apparent viscosity of the slurry to

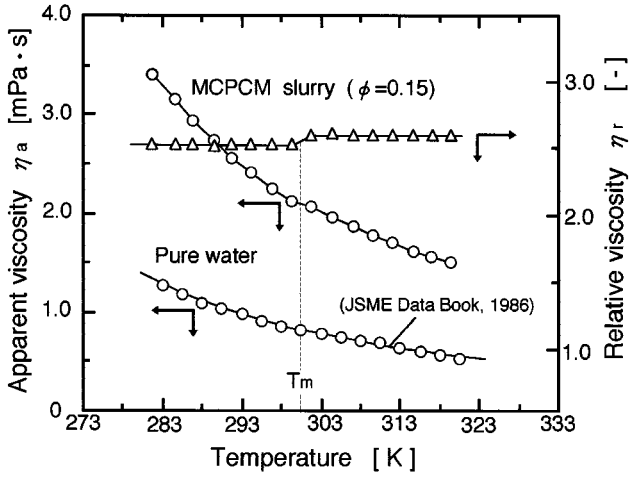

Figure 5. Effect of temperature on apparent and relative viscosity for MCPCM slurry.

Results of Couette viscometer measurement for the shear rate of 100 s^{-1} and the gap size of 1.27 mm.

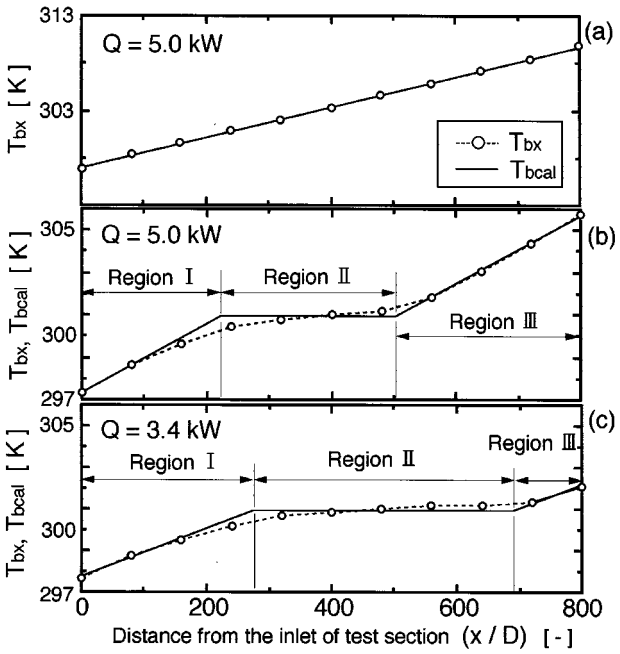

Figure 6. Measured bulk mean temperature T_{bx} and calculated temperature for (a) pure water and (b,c) MCPCM slurry of $\phi = 0.12$ at the same mean flow velocity of $\bar{u} = 1.25$ m/s.

the viscosity of pure water, remains constant. The change in the apparent viscosity of the slurry with temperature was strongly correlated with the change in the viscosity of pure water. At the melting temperature of octadecane, a nominal change of approximately 3% in the relative viscosity was shown because of the volume change of PCM. This change was not clearly reflected in the pressure-drop data, however, and therefore no significant change in pressure drops related to the melting of MCPCMs was found when the test-section wall was heated.

In Figure 3, it is interesting to note that the pressure drops for $\phi = 0.3$ are lower than those for pure water in the mean flow velocity range of 2.0–2.5 m/s. This is because the increased slurry viscosity caused the laminarization of the slurry flow. A similar effect of fine particles on the turbulence of slurry flow was also reported previously (Abbas and Crowe, 1987; Lui et al., 1988). It is believed that the longitudinal eddy diffusivity of a slurry flow is depressed when the geometrical dimensions of the particles are smaller than the turbulence length scale. This pressure-drop reduction relative to the case of a single-phase fluid is useful for the slurry system in respect to the reduction in pumping power because an MCPCM slurry of higher particle fraction, and with larger thermal capacity, can be conveyed with a lower pressure drop relative to conventional single-phase heat-transfer fluids.

Heat-transfer characteristics

Figure 6 shows the profiles of local bulk mean temperature, T_{bx}, measured along the test section for the turbulent flow of pure water and MCPCM slurry of $\phi = 0.12$. Both fluid

flows had the same mean flow velocity of 1.25 m/s. For pure water (Figure 6a), the local bulk mean temperature increases linearly along the flow direction because of uniform heating in all the segments. The heating rate, Q, of 5.0 kW was the total value in the overall test section when all the segments were heated. Energy-balance calculations comparing the electrical-power input with the thermal energy removed by pure water consistently showed that there was a heat loss of about 10% of the electrical-power input in every segment. For this reason, the heating rate Q or the local heat flux q_{wx} were corrected by a uniform 10% decrease in the measured electrical power input. For a slurry with the same heating rate (Figure 6b), the profile is not linear because of the energy absorption associated with PCM melting. The overall temperature rise in the test section is smaller than that of pure water under the same heating-rate condition because the slurry has greater thermal capacity. Figure 6c shows that the melting of MCPCMs occurs at a far axial distance as the heating rate decreases (that is, $Q = 3.4$ kW). Either the flow rate or the heating rate should be adjusted so that all the solid MCPCM particles in the slurry can melt within a test section of limited length.

In Figure 6a–6c, the measured temperatures, T_{bx}, are compared with calculated temperatures, $T_{b\text{cal}}$, represented by solid lines. The temperatures and the lengths of regions I–III in Figure 6b and 6c were calculated using energy-balance equations (Choi et al., 1994). It is assumed that the temperatures in Region II are fixed at the melting temperature of octadecane. In regions I and III, the thermal energy applied from the tube wall is assumed to balance with the sensible heat of the slurry, that is, the latent heat of slurry is neglected. Choi et al. (1994) also employed a similar model to predict the local bulk mean temperature of turbulent slurry flow. Furthermore, this model is based upon the following assumptions: (1) the particle size is small enough for particles to melt or solidify instantaneously, (2) MCPCM has no supercooling, and (3) there is good mixing by turbulence of the flow at every cross section. The T_{bx} profiles approximately coincide with those of $T_{b\text{cal}}$. However, these assumptions could not actually be met for the MCPCM particles because of the MCPCM supercooling phenomenon and finite melting rates. Therefore, there was a slight deviation of the measured temperature from the calculated temperature, as is shown in the figures. The measured temperature is lower than the calculated temperature in the range where the wall temperature, T_w, is higher and local temperatures in a turbulent core region are lower than the melting temperature (region I). This is because the assumptions in calculated temperature implicitly include the resolidification process of melted MCPCMs (an energy-release process), while the MCPCMs exhibit the supercooling phenomenon. In regions II and III, on the other hand, the high heating rate from the tube wall would exceed the energy-absorption rate of melting because of the finite melting rates of MCPCMs. This results in a higher measured temperature relative to the calculated temperature. It should be noted that the measured temperature corresponds to a "mixed mean" temperature (that is, the temperature which can be estimated from an integral heat balance) and not a "flow weighted" bulk temperature (that is, the mean temperature that can be obtained only from the local temperatures as a given cross section). Furthermore, the measured temperature is thought to be more accurate because the effects of supercooling and finite melting rate on the mixed mean temperature are taken into account. Although these bulk mean temperatures are essentially equivalent for a single-phase fluid, it is likely that they are different for a phase-change slurry. For example, when the solid particles melt at an overall cross section of the tube, the temperatures of the suspending fluid at that cross section can be greater than the melting temperature. In this case, the flow-weighted bulk temperature will be greater than the melting temperature. On the other hand, if the particles melt instantaneously at the melting temperature, the mixed mean temperature will be equal to the melting temperature because the increase in the heat of the suspending fluid will easily balance with the progress of melting.

In previous experimental studies (Goel et al., 1994; Choi et al., 1994), the local bulk mean temperatures for a phase-change slurry have not been measured. The heat-transfer performance of phase-change slurry has been discussed only on the basis of heat-transfer coefficients estimated from calculated temperature using the previously mentioned model. As a result, there does not seem to be a consensus on the issue of how to define the bulk mean temperature suitable for such fluids. Goel et al. (1994) reported that melting of MCPCMs in a laminar slurry flow actually occurred over a range of temperatures around the melting temperature of PCM and pointed out that the varying melting temperatures would affect the estimation of the heat-transfer coefficient. The heat-transfer coefficient defined from the measured temperature is thought to be more useful for the evaluation of heat-transfer performance of MCPCM slurry with phase change. In the strict sense, however, it is very difficult to measure the mixed mean temperature for the slurry flow because the melting of particles can occur even in the nonheated end part of the test section and the mixing chamber when the measured temperatures are greater than the melting temperature. This results in a decrease in the mixed mean temperature, and therefore an underestimation in the heat-transfer coefficient (Eq. 3). If the residence time of solid particles in the mixing chamber is long enough for the slurry to achieve a thermal-equilibrium state, the measured temperatures will always be equal to the melting temperature, except where the effect of supercooling on the mixed mean temperature will be exhibited.

Figure 7a and 7b show the measured bulk mean temperatures, T_{bx}, and the corresponding local heat-transfer coefficients, h_x, for the turbulent flows of pure water and slurry of $\phi = 0.12$, respectively. As is shown Figure 7b, the local heat-transfer coefficients for the pure-water flow increase slightly along the flow direction, because the degree of turbulence increases as the viscosity of water decreases with temperature. In the case of a slurry flow at the same mean flow velocity, the local heat-transfer coefficients are lower than those for a pure-water flow near the test-section inlet and outlet ($x/D = 40$ and 760), where the effect of latent heat would be negligible. This degradation of heat-transfer performance relative to a single-phase fluid flow can be caused by the decrease in degree of turbulence associated with the increased slurry viscosity. The local Reynolds numbers at the inlet and outlet of the test section, calculated from the viscosities corresponding to the measured temperatures, are given in Fig-

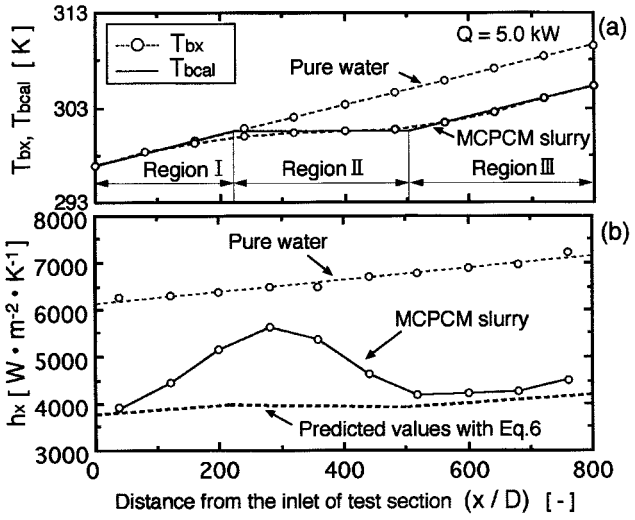

Figure 7. (a) Bulk mean temperature vs. (b) local heat-transfer coefficient for pure water and MCPCM slurry of $\phi = 0.12$.

$Re_{bx} = 14{,}230-17{,}865$ for pure water and $Re_{bx} = 7360-8650$ for MCPCM slurry, at $\bar{u} = 1.25$ m/s.

ure 7b. In regions I and II, however, a significant variation in the local heat-transfer coefficient is shown. The local heat-transfer coefficients increase in region I and approach those for the pure-water flow.

The dashed line in Figure 7b shows the local heat-transfer coefficients calculated by using the following formula, which was presented by Choi and Cho (1995) for the turbulent convective heat transfer of a single-phase fluid with high heat flux:

$$Nu_x = 0.00425 Re_{bx}^{0.979} Pr_{bx}^{0.4} (\eta_{wx}/\eta_{bx})^{-0.11}. \qquad (6)$$

Here, the local Reynolds number, Re_{bx}, and local Prandtl number, Pr_{bx}, were calculated on the basis of the local bulk mean temperatures of the fluid, and the change in physical properties along the axial direction of the test section was taken into account. The performance of our experimental system was repeatedly checked with pure water, and the maximum relative discrepancies between predicted values and experimental data were found to be within 15% in the local Nusselt number, Nu_x, over the Reynolds number range of 3,000 to 20,000 and in the heating rate range of 2 to 15 kW. Further details of the experimental accuracy are given by Yamagishi et al. (1998b). For the MCPCM slurry flow, the dashed line in Figure 7b represents the values that were also predicted using Eq. 6, assuming that the slurry is a Newtonian homogeneous fluid that involves no phase change. The details of the assumptions are given in Appendix B. When the experimental data for the slurry are compared with the predicted values, the data in region III are close to the predicted values and increase gradually along the flow direction because of the axial viscosity change. In regions I and II, on the other hand, there is a considerable deviation of the experimental data from the predicted values, which can be attributed to the effect of phase change on the effective specific heat of the slurry (Eq. 2).

Lui et al. (1988) reported that the average heat-transfer coefficients decreased with the fraction of polyethylene particles of 1.3 mm in diameter in the slurry under a fixed flow-rate condition, where no phase change was involved in the slurry. In addition, as for the effect of phase change on turbulent heat transfer, Choi et al. (1994) also reported that a significant variation in the local heat-transfer coefficient was found in the flow of hexadecane–water slurry when the solid hexadecane particles were melting in a circular tube under a uniform heat-flux condition. In their study, furthermore, the local pressure drops were found to decrease significantly at the point where the solid particles melted, because the solid–liquid phase of suspension changed to the liquid–liquid phase of emulsion. Although such a significant change in local pressure drop was not detected in the present study using the MCPCM slurry, the heat-transfer analogies for the MCPCM slurry may still be similar to the case for PCM slurry because there is no reason to suppose that the melting process of MCPCM is different from that of PCM particles. Choi et al. (1994) speculated that the variation in the local heat-transfer coefficient would depend upon the number of solid PCM particles that migrated from the turbulent core region to the flow fields near the heated tube wall and melted. The inner-wall temperature, T_w, decreased because the slurry temperature near the tube wall decreased when the PCM melted, resulting in an increase in the local heat-transfer coefficient (Eq. 3). Based on the pressure-drop change, they also speculated that a boundary layer of fully melted particles exists near the heated test-section wall. In their study, however, such flow parameters as PCM fractions in the slurry and the flow rates were not varied in order to prove these speculations.

As is shown in Figure 7b, the local heat-transfer coefficients increase in region I, where the measured bulk mean temperatures were lower than the melting temperature of octadecane. This phenomenon can be explained as follows: (1) the temperatures at the flow fields near the heated tube wall are higher than the melting temperature, while the slurry temperatures in the turbulent core region are lower; (2) the solid MCPCM particles migrating from the turbulent core region to the tube wall can melt when the temperature of the particles increased beyond the melting temperature; and (3) the solid particles would have a greater possibility to melt as the slurry temperature in the turbulent core as well as the measured bulk mean temperature approached the melting temperature. As a result, the number of solid particles melting near the tube wall increased with measured temperature, resulting in an increase in the local heat-transfer coefficient. In region II, on the other hand, the local heat-transfer coefficients decreased because the number of solid MCPCMs in the slurry eventually decreased.

Figure 8 shows a comparison of slurry flows under different heating rates, Q, of 5.0 and 8.8 kW. The particle fractions in the slurry, the mean flow velocities, and the slurry temperatures at the test-section inlet were identical for both cases ($\phi = 0.12$, $\bar{u} = 1.54$ m/s, $T_{bi} = 297$ K). It should be noted that the maximum value of local heat-transfer coefficient for $Q =$ 8.8 kW is lower than that for $Q = 5.0$ kW. If the heat-transfer augmentation associated with phase change as defined by the difference between the value near the test-section inlet (that is, $x/D = 40$) and the maximum value, the augmentation de-

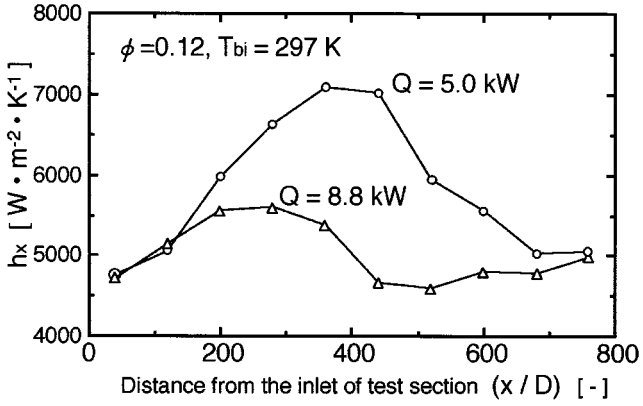

Figure 8. Local heat-transfer coefficients for MCPCM slurry with different heating rates of 5.0 and 8.8 kW.

Re_{bx} = 9311–11,020 for Q = 5.0 kW, and Re_{bx} = 9325–12,535 for Q = 8.8 kW, at $\bar{u}$ = 1.54 m/s.

creases as the heating rate increases. This phenomenon can be explained as follows: (1) when the heating rate became higher, the thickness of the boundary layer of fully melted particles would become thicker, and (2) the solid particles migrating from the turbulent core to the tube wall would melt at a far radial distance from the tube wall. The increased heating rate results in prevention of the transport of solid PCM particles to the tube wall. Choi et al. (1994) also reported a similar effect of heating rate on augmentation of the local heat-transfer coefficient.

Figure 9 shows a comparison between the profiles of local heat-transfer coefficient for slurry flows (a)–(d) of different Reynolds numbers. The slurry temperatures at the test-section inlet and the heating rates were equal for all cases (that is, T_{bi} = 297 K, Q = 5.0 kW). The particle volume fractions, ϕ, and the mean flow velocities, $\bar{u}$, were varied to obtain approximately the same Reynolds numbers in flows (a) and (b), or in (c) and (d). The results show that the slurry with a higher MCPCM fraction has a higher maximum value of the local heat-transfer coefficient at the same Reynolds number, that is, the same degree of turbulence. This is in agreement with Eq. 2. On the other hand, when flows (b) and (c) at approximately the same mean flow velocity are compared, the flow (c) of the higher particle fraction of ϕ = 0.15 has a lower heat-transfer augmentation. In this case, the flow (b) of ϕ = 0.07 had the higher Reynolds numbers (Re_{bx} = 11,094–12,962) than that of the flow (c) (that is, Re_{bx} = 5,294–6,329). The increased slurry viscosity would impede the radial migration of solid MCPCM particles associated with the turbulent fluid motion. This results in a decrease in the number of solid MCPCM particles melting near the tube wall, and therefore the heat-transfer augmentation decreases. This augmentation can also be related to the slurry flow behavior. For a relatively high particle fraction, this effect of turbulent flow behavior on heat-transfer augmentation would be dominant compared with the immediate effect of PCM fractions on the effective specific heat, which can be attributed to the previously mentioned nonlinear relationship between slurry viscosity and particle volume fraction.

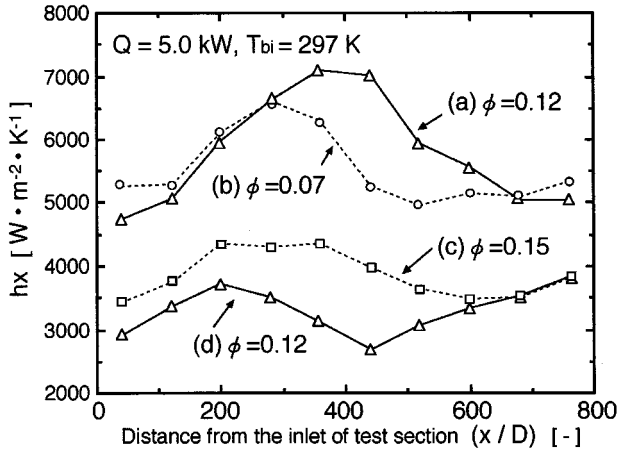

Figure 9. Local heat-transfer coefficients of MCPCM slurries for different Reynolds numbers.

(a) Re_{bx} = 9,311–11,020 at $\bar{u}$ = 1.54 m/s for ϕ = 0.12; (b) Re_{bx} = 11,094–12,962 at $\bar{u}$ = 1.35 m/s for ϕ = 0.07; (c) Re_{bx} = 5,294–6,329 at $\bar{u}$ = 1.25 m/s for ϕ = 0.15; (d) Re_{bx} = 5,488–6,495 at $\bar{u}$ = 0.91 m/s for ϕ = 0.12.

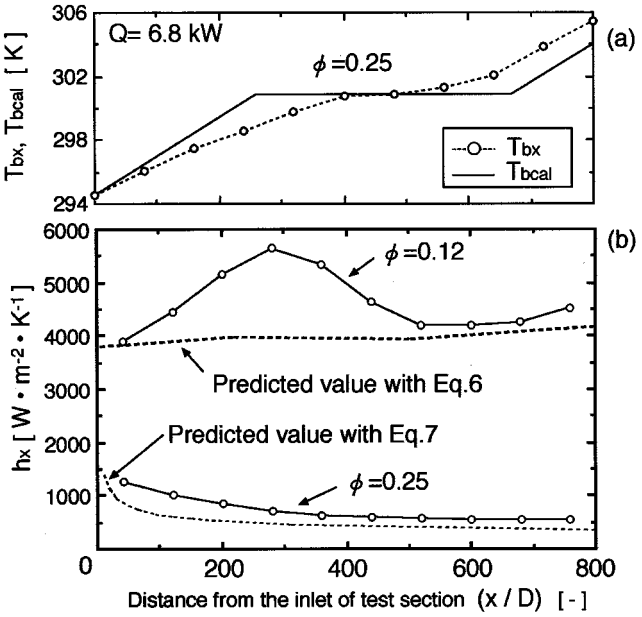

Figure 10. (a) Bulk mean temperature and (b) local heat-transfer coefficient profiles for MCPCM slurries of ϕ = 0.12 and 0.25.

Re_{bx} = 7,360–8,650 ($\bar{u}$ = 1.25 m/s) with Q = 5.0 kW for ϕ = 0.12; Re_{bx} = 1,696–2,183 ($\bar{u}$ = 1.22 m/s) with Q = 6.8 kW for ϕ = 0.25.

Figure 10a and 10b show the profiles of bulk mean temperatures and the local heat-transfer coefficients for slurry of ϕ = 0.25 ($\bar{u}$ = 1.25 m/s, Q = 6.8 kW), respectively. In this flow condition (that is, Re_{bx} = 1,696–2,183), the pressure-drop reduction relative to pure water mentioned earlier was found because of laminarization. Figure 10a shows that the measured temperature, T_{bx}, deviated noticeably from the calculated temperature, T_{bcal}, even at the test-section outlet. In this case, the melting of all the solid particles was not com-

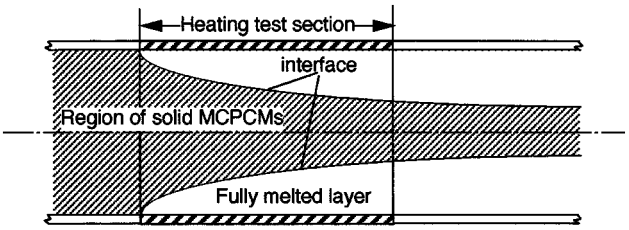

Figure 11. Postulated melting process in a laminar flow.

pleted in the overall test section. This problem can be related to the melting process of MCPCM particles in a laminar slurry flow, which can be postulated as follows: (1) a layer of fully melted particles develops from the wall to the core of tube concentrically along the flow direction (Figure 11), and (2) the MCPCM melting occurs only around the interface between this layer and the region of solid particles. The radial distance from the tube wall to the interface at the end of the heated test section can be highly dependent upon the melting rates of solid particles at the interface, as well as the heat conduction rate of fully melted slurry. Because the temperatures at the interface are constant at the melting temperature, the temperatures of the fully melted slurry can increase beyond the melting temperature, resulting in increasing the sensible heat of the melted slurry. This increase in the sensible heat is necessary for the progress of the melting in the laminar slurry flow. As a result, it is possible that the solid particles in the laminar slurry flow are not completely melted because of the energy balance, which is contrary to our expectation. Mulligan et al. (1994) also reported that a similar problem of incomplete melting occurred in the laminar slurry flows. The relatively large differences between measured and calculated temperatures can be related to the effect of either supercooling or finite melting rates of MCPCM particles, as was described before. The melted particles that originated from the fully melted layer could not resolidify in the mixing chamber because of the supercooling of MCPCM. Furthermore, the particle fraction in the laminar slurry flow was higher than that for the turbulent flow. In addition, because the sensible heat of the melted slurry was increased significantly, the residence time of the solid particles in the mixing chamber would not be long enough to reduce the measured bulk mean temperature to the melting temperature. In this case, a uniform distribution of slurry temperatures in the mixing chamber has been obtained.

In Figure 10b, the local heat-transfer coefficients for $\phi = 0.25$ are compared to those for the turbulent flow (that is, $\phi = 0.12$, $\bar{u} = 1.25$ m/s, $Q = 5.0$ kW). The local heat-transfer coefficients are much lower than those for the turbulent flow in the overall test section, though the particle fraction was higher. The predicted values for $\phi = 0.25$ in Figure 10b were calculated using Eq. 7, neglecting the effect of latent heat for the local Nusselt number of the fully developed single-phase Newtonian laminar flow in the thermally developing region (Shah and London, 1978), as

$$Nu_x = 5.364\left[1 + (220\,x^+/\pi)^{-10/9}\right]^{3/10} - 1.0,$$

where

$$x^+ = (x/D)/(Re_{bx} \cdot Pr_{bx}). \tag{7}$$

Similar to the prediction for the turbulent flow, local Reynolds numbers and local Prandtl numbers were calculated from the physical properties corresponding to the calculated temperature, T_{bcal}. The effect of radial viscosity change was corrected by using the factor $(\eta_{bx}/\eta_{wx})^{0.14}$ (Sieder and Tate, 1936). As is shown in the figure, the experimental data have the same trend as that of the predicted values. The numerical simulation developed by Charunyakorn et al. (1991) also showed that the local Nusselt number or the local heat-transfer coefficient was maximum at the inlet of a circular heating duct and decreased along the flow direction with a trend that was the same as that for a single-phase flow, where the slurry temperature at the inlet was assumed to be the melting temperature of PCM. The heat-transfer augmentation for the laminar slurry flow was difficult to be evaluated because it was indistinguishable from the change in the heat-transfer coefficients associated with the entrance effect for the developing laminar flow. Furthermore, the augmentation due to phase change may not be evaluated adequately by varying such parameters as the particle volume fractions and the mean flow velocities because there are some uncertainties associated with the incomplete melting of the solid particles; nevertheless, if the particle volume fractions are the same for both laminar and turbulent flows, it can be concluded that the heat transfer in the turbulent flow is more effective than that in the laminar flow, even when the slurries undergo phase change.

Discussion of system design

The results just given show that the heat-transfer performance of MCPCM slurry is strongly related to the flow conditions. A turbulent heat transfer was more effective compared with the case of a laminar flow. Therefore, a turbulent slurry flow is desirable for the heat-exchange operation. On the other hand, the pressure-drop reduction relative to a single-phase fluid was found because of the flow-structure change from turbulent to laminar. The laminar slurry flow with a high load of MCPCM particles benefits from a high-energy transportation density, reduced pumping power, and reduced heat loss in comparison to the case of a system using a single-phase working fluid. In view of these trade-offs, it is important for the system design to define the flow regime where beneficial effects are presented, though the system may possibly need special equipment for particle-load control.

When the MCPCMs in the slurry melted, the local heat-transfer coefficients for the turbulent flows were found to increase, and this phenomenon compensated the heat-transfer degradation associated with the increased slurry viscosity relative to the viscosity of a single-phase fluid. The heat-transfer augmentation associated with phase change was found to depend upon not only the fraction of solid particles in the slurry but upon the degree of turbulence and the heating rate in the heat exchanger. The effective specific heat, Cp_{eff}, in Eq. 2 can also be a function of these parameters.

Based on the experimental data, considering Figure 9, the effective specific heat was increased by approximately 2.7 times, which was calculated from the maximum of local heat-transfer coefficients for the slurry flow ($\phi = 0.12$, $\bar{u} =$ 1.54 m/s, $Q = 5.0$ kW) using Eq. 1. A potential increase in the effective specific heat for a certain application, however, cannot be predicted directly by the extrapolation from the present data because the heat-transfer augmentation highly depends upon the motions of MCPCM particles in the turbulent boundary layer, as well as the phase-change rates of MCPCM particles. This prediction for the turbulent flow is much more complex as compared with the laminar flow case. Furthermore, the investigations of such particle motions, either theoretical or experimental, are almost lacking, and the existing data for such a phenomenon are quite incomplete. In the present study, unfortunately, the local heat-transfer coefficients for the turbulent flow of MCPCM slurry with phase change were not greater than those for the flow of pure water at the same mean flow velocity because high heating rates from the tube wall were necessary for the complete melting of the slurry within the limited-length test section, and therefore, a large increase in the effective specific heat was difficult to achieve. However, if a moderate condition of heating rate is available for a practical application, the local heat-transfer coefficients for the slurry flows is likely to outweigh those for single-phase fluids. In addition, it is clear that the slurry of MCPCMs with larger latent heat, higher phase-change rate, and no supercooling promises to have a more effective heat-transfer performance. As a result, the present experimental data can give design criteria for a thermal-energy transportation system using MCPCM slurry.

Conclusions

The results presented in this article show the hydrodynamic and heat-transfer characteristics of MCPCM slurry as a heat-transfer fluid. The highlights of the experimental results can be summarized as follows.

1. The results of pressure-drop measurement showed that the flow structure of MCPCM slurry changed from turbulent to laminar as the particle volume fractions in the slurry were increased under a constant flow-rate condition. The pressure-drop reduction relative to pure water was found for a laminarized slurry flow.

2. The local bulk mean temperatures of the MCPCM slurry flows were measured. When the melting of MCPCM particles occurred, these temperatures were found to change in a range across the melting temperature of octadecane because of the supercooling and finite melting rates of MCPCM particles.

3. In the case of a turbulent flow, the local heat-transfer coefficients increased when MCPCMs melted. The maximum value of the local heat-transfer coefficient was found to depend upon the PCM fraction in the slurry, the degree of turbulence and the heating rate in the test section.

4. In the case of a laminarized slurry flow, the heat-transfer performance was found to degrade compared with that of a turbulent flow. The problem associated with incomplete melting of slurry in the heat-transfer test section was pointed out.

Acknowledgment

This work was supported by the New Energy and Industrial Technology Development Organization (NEDO) as a part of the New Sunshine Project under the Ministry of International Trade and Industry (MITI), Japan. The authors thank Mr. Shojiro Sagiya and Mr. Masayuki Nakanishi of Japan Capsule Products, Inc., for their technical advice in the preparation of microcapsules.

Literature Cited

Abbas, M. A., and C. T. Crowe, "Experimental Study of the Flow Properties of a Homogeneous Slurry Near Transitional Reynolds Numbers," *Int. J. Multiphase Flows*, **13**, 357 (1987).

Aude, T. C., N. T. Cowper, T. L. Thompson, and E. J. Wasp, "Slurry Piping Systems: Trends, Design Methods, Guidelines," *Chem. Eng.*, 74 (1971).

Bahrami, P. A., "Fusible Pellet Transport and Storage of Heat," ASME Paper No. 82-HT-32 (1982).

Charunyakorn, P., S. Sengupta, and S. K. Roy, "Forced Convection Heat Transfer in Microencapsulated Phase Change Material Slurries: Flow in Circular Ducts," *Int. J. Heat Mass Transfer*, **34**, 819 (1991).

Chen, K., and M. M. Chen, "An Analytical and Experimental Investigation of the Forced Convective Heat Transfer of Phase-Change Slurry Flows," *Proc. Int. Symp. Multiphase Flows* (*II*), Ziejiang Univ. Press, China, p. 496 (1987).

Choi, E., Y. I. Cho, and H. G. Lorsch, "Forced Convection Heat Transfer with Phase-Change-Material Slurries: Turbulent Flow in a Circular Tube," *Int. J. Heat Mass Transfer*, **37**, 207 (1994).

Choi, E., and Y. I. Cho, "Local Friction and Heat Transfer Behavior of Water in a Turbulent Pipe Flow with Large Heat Flux at the Wall," *J. Heat Transfer*, **117**, 283 (1995).

Clearly, C., S. Day, R. Lindsay, C. Murry, R. Gupta, B. Larkin, H. Thompson, M. Wiggin, and J. S. O' C. Young, "Hydraulic Characteristics of Ice Slurry and Chilled Water Flows," *IEA District Heating: Advanced Energy Transmission Fluid-Final Report of Research*, Novem BV, Sittard, Netherlands (1990).

Colvin, D. P., and J. C. Mulligan, "Spacecraft Heat Rejection Methods: Active and Passive Heat Transfer for Electronic Systems," Phase I, Final Rep., AFWAL-TR-86-3074 (1986).

Colvin, D. P., J. C. Mulligan, and Y. G. Bryant, "Enhanced Heat Transport in Environmental Systems Using Microencapsulated Phase Change Materials," *Proc. Int. Conf. Environmental Systems*, Seattle, WA, p. 717 (1992).

Darby, R., "Hydrodynamics of Slurry and Suspensions," *Encyclopedia of Fluid Mechanics*, N. P. Cheremisinoff, ed., Vol. 5, Gulf Pub., Houston (1986).

Dodge, D. W., and A. B. Metzner, "Turbulent Flow of Non-Newtonian Systems," *AIChE J.*, **5**, 189 (1959).

Eveson, G. F., "The Rheological Properties of Stable Suspensions of Very Small Spheres at Low Rates of Shear," *J. Oil Colour Chem. Assoc.*, **40**, 456 (1957).

Goel, M., S. K. Roy, and S. Sengupta, "Laminar Forced Convection Heat Transfer in Microencapsulated Phase Change Material Suspensions," *Int. J. Heat Mass Transfer*, **37**, 593 (1994).

Guyer, E. C., and D. L. Brownell, *Handbook of Applied Thermal Design*, McGraw-Hill, New York (1988).

Hart, R., and F. Thornton, "Microencapsulation of Phase Change Materials," Final Rep., DOE Contract No. 82, 80, Ohio (1982).

Holman, J. P., *Heat Transfer*, 5th ed., McGraw-Hill, New York, p. 174 (1981).

JSME, JSME Data Book, *Heat Transfer*, 4th ed., Maruzen, Tokyo, Japan, p. 331 (1986).

Kasza, K. E., and M. M. Chen, "Improvement of the Performance of Solar Energy for Waste Heat Transfer/Storage Fluid," *Proc. ASME 6th Ann. Solar Energy Div. Conf.*, Las Vegas, NV, p. 166 (1984).

Lui, K. V., U. S. Choi, and K. E. Kasza, "Pressure Drop and Heat Transfer Characteristics of Nearly Neutrally Buoyant Particulate Slurry for Advanced Energy Transmission Fluids," *ASME Fluids Eng. Div.*, **75**, 107 (1988).

Maxwell, J. C., *A Treatise on Electricity and Magnetism*, 3rd ed., Vol. 1, Dover, New York, p. 440 (1954).

McMahon, W. A., Jr., W. W. Harlowe, Jr., and D. J. Mangold, "Feasibility Study of Utilizing Phase Change Coolant for Protective Garment," Final Rep., Contract No. DAAK 60-81-C-0098, U.S. Army Natick Research and Development Command, MA (1982).
Mehalick, E. M., and A. T. Tweedie, "Two Component Thermal Energy Storage Material," Rep. NSF/RANN/AE/AER-74-09186, National Science Foundation, Washington, DC (1975).
Mulligan, J. C., D. P. Colvin, and Y. G. Bryant, "Use of Two-Component Fluids of Microencapsulated Phase-Change Materials for Heat Transfer in Spacecraft Thermal Systems," AIAA Paper No. 94, 2004 (1994).
Park, J. T., T. A. Grimely, and R.J. Mannheimer, "LDV Velocity Profile Measurements of a Non-Newtonian Slurry with Various Yield Stress in Turbulent Pipe Flow," *Proc. Int. Conf. Multiphase Flow*, IF-24, Kyoto, Japan (1995).
Roff, W. J., J. R. Scott, and J. Pacitti, *Handbook of Common Polymers*, CRC Press, Cleveland (1971).
Roy, S. K., and S. Sengupta, "An Evaluation of Phase Change Microcapsules for Use in Enhanced Heat Transfer Fluids," *Int. Commun. Heat Mass Transfer*, **18**, 495 (1991).
Schlichting, H., *Boundary Layer Theory*, 4th ed., McGraw-Hill, New York (1960).
Shah, R. K., and A. L. London, *Advance in Heat Transfer*, Academic Press, New York (1978).
Shon, C. W.,and M. M. Chen, "Heat Transfer Enhancement in Laminar Slurry Pipe Flows with Power Law Thermal Conductivities," *J. Heat Transfer*, **106**, 539 (1984).
Sieder, E. N., and G. E. Tate, "Heat Transfer and Pressure Drop of Liquids in Tubes," *Ind. Eng. Chem.*, **28**, 1429 (1936).
The Society of Thermophysical Properties, *Thermophysical Properties Handbook*, Youkendo, Tokyo, (1994).
Vand, V., "Theory of Viscosity of Concentrated Suspension," *Nature*, **155**, 364 (1945).
Winters, P. J., "Phase Two Laboratory Testing of Direct Freeze Ice Slurry District Cooling," Final Rep., DOE Contract No. DE-FG01-88CE26559 (1991).
Yamagishi, Y., T. Sugeno, T. Ishige, H. Takeuchi, and A. T. Pyatenko, "An Evaluation of Microencapsulated PCM for Use in Cold Energy Transportation Medium," *Proc. IECEC*, Washington, DC, p. 2077 (1996).
Yamagishi, Y., T Sugeno, H. Takeuchi, and A. T. Pyatenko, "Thermal Characteristics of Supercooled Phase Change Materials Inside Microcapsules," *Netsu Bussei*, **12**(1), 24 (1998a).
Yamagishi, Y., T. Sugeno, H. Takeuchi, and A. T. Pyatenko, "Forced Convection Heat Transfer with Microencapsulated Phase Change Material Slurries—Turbulent Flow in a Circular Tube," *Kagaku Kogaku Ronbunshu*, **24**(1), 104 (1998b).
Yamane, H., and H. Ohshima, and T. Kondo, "Freezing Behavior of Microencapsulated Water," *J. Microencapsulation*, **9**(3), 279 (1992).

Appendix A: Physical Properties

The density and the specific heat of a slurry or an MCPCM particle are calculated on the basis of mass or energy balance. The weight fraction, c, of each material in slurry was determined before the slurry manufacturing process. For example, the specific heat, Cp, of the slurry is given by

$$Cp_b = c_{\text{pcm}} Cp_{\text{pcm}} + c_{cw} Cp_{cw} + \left(1 - c_{\text{pcm}} - c_{cw}\right) Cp_f. \quad \text{(A1)}$$

The thermal conductivity, k, of the MCPCM slurry is calculated from Maxwell's relation (1954) for the bulk thermal conductivity of static suspension with conductivities of the same order for the suspending and the dispersed media.

$$k_b = k_f \cdot \frac{2k_f + k_p + 2\phi\left(k_p - k_f\right)}{2k_f + k_p - \phi\left(k_p - k_f\right)}, \quad \text{(A2)}$$

where the thermal conductivity of an MCPCM particle is calculated by using the composite sphere approach (Goel et al., 1994; Guyer and Brownell, 1988) and given by

$$\frac{1}{k_p d_p} = \frac{1}{k_{\text{pcm}} d_{\text{pcm}}} + \frac{d_p - d_{\text{pcm}}}{k_{me} d_p d_{\text{pcm}}}. \quad \text{(A3)}$$

Appendix B: Prediction of Local Heat-Transfer Coefficient

The predicted values in Figures 7b and 10b were calculated using Eqs. 6 or 7. The local Reynolds number and the local Prandtl numbers were calculated from the physical properties given in Table 1. Then the change in the slurry viscosity with temperature was taken into account in the following manner. The slurry viscosity η_b was calculated from the viscosity of pure water η_f corresponding to a calculated temperature $T_{b\text{cal}}$, assuming that the relative viscosity η_r was a constant value independent of temperature; that is, $\eta_b = \eta_r \cdot \eta_f$. The relative viscosity was determined from the slurry viscosity given in Table 1. To calculate the slurry viscosity at the inner tube wall temperature, η_w, the wall temperature T_w at any distance from the inlet of the test section was calculated from a linear interpolation, including the two adjacent temperatures that were measured discretely along the test section.

Manuscript received Oct. 19, 1998, and revision received Feb. 1, 1999.